Signal Processing Assignment

Donald Carr

May 18, 2005

Question 1

Common facts

My -3 dB frequency was : 2 kHz
$\therefore \omega_c = 2\pi 2000$

The circuits were taken from the Electronic Filter Design Handbook (Williams, 1981). Standard values were acquired for the respective configurations and denormalised accordingly using the FSF and Z adjustment.

"Π" CLC

$R_s = 600\ \Omega$
$C_1 = 0.132\ \mu$F
$L_2 = 95.5$ mL
$C_3 = 0.132\ \mu$F
$R_o = 600\ \Omega$

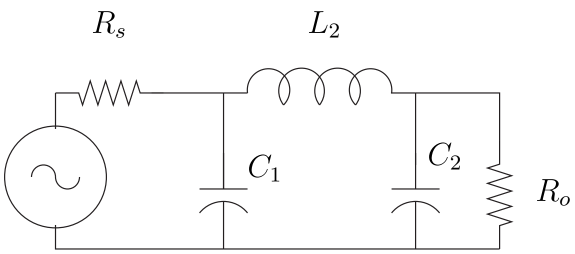

Figure 1: The "π" CLC circuit

"T" LCL

$R_s = 600\ \Omega$
$L_1 = 0.048$ mL
Standard values were acquired $C_2 = 0.265\ \mu$F
$L_3 = 0.048$ mL
$R_o = 600\ \Omega$

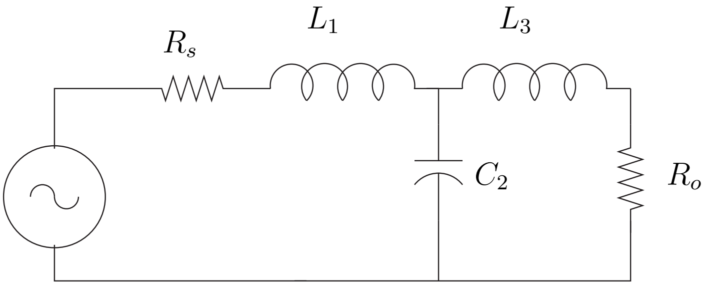

Figure 2: The "T" LCL circuit

Question 2 : The T configuration

Matrix loop equation

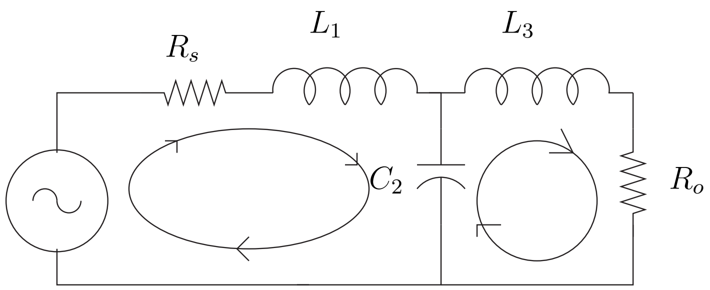

Figure 3: The "T" LCL circuit

For the sake of convenience I have dropped the explicit time dependence from the terms. Similarly, I have dropped the explicit s dependence of the terms following the Laplace transform.

Loop 1

$$\begin{aligned}
\sum v = 0 &= v_{Rs} + v_{L1} + v_{C2} - u \\
0 &= i_1 R_s + L_1 \frac{di_1}{dt} + \frac{1}{C_2}\int_0^t (i_1 - i_2) d\tau + v(0) - u \\
0 &= \frac{di_1}{dt} R_s + L_1 \frac{d^2 i_1}{dt} + \frac{1}{C_2}(i_1 - i_2) - \frac{du}{dt} \\
=> 0 &= sI_1 R_s + L_1 s^2 I_1 + \frac{1}{C_2}(I_1 - I_2) - sU \text{ (Laplace)} \\
0 &= I_1 R_s + L_1 s I_1 + \frac{1}{sC_2}(I_1 - I_2) - U \\
U &= (R_s + sL_1 + \frac{1}{sC_2}) I_1 - \frac{1}{sC_2} I_2
\end{aligned}$$

Loop 2

$$\begin{aligned}
\sum v = 0 &= v_{Ro} + v_{L3} - v_{C2} \\
0 &= i_2 R_o + L_3 \frac{di_2}{dt} - \frac{1}{C_2}\int_0^t (i_1 - i_2) d\tau - v(0) \\
0 &= \frac{di_2}{dt} R_o + L_3 \frac{d^2 i_2}{dt} - \frac{1}{C_2}(i_1 - i_2) d\tau \\
=> 0 &= sI_2 R_o + L_3 s^2 I_2 - \frac{1}{C_2}(I_1 - I_2) d\tau \text{ (Laplace)} \\
0 &= I_2 R_o + L_3 s I_2 - \frac{1}{sC_2}(I_1 - I_2) d\tau
\end{aligned}$$

$$0 = \frac{-1}{sC_2}I_1 + (R_o + sL_3 + \frac{1}{sC_2})I_2$$

$$\begin{bmatrix} R_s + sL_1 + \frac{1}{sC} & \frac{-1}{sC} \\ \frac{-1}{sC} & R_o + sL_3 + \frac{1}{sC} \end{bmatrix} \begin{bmatrix} I_1 \\ I_2 \end{bmatrix} = \begin{bmatrix} U \\ 0 \end{bmatrix}$$

$$\begin{bmatrix} I_1 \\ I_2 \end{bmatrix} = \begin{bmatrix} R_s + sL_1 + \frac{1}{sC} & \frac{-1}{sC} \\ \frac{-1}{sC} & R_o + sL_3 + \frac{1}{sC} \end{bmatrix}^{-1} \begin{bmatrix} U \\ 0 \end{bmatrix}$$

$$\therefore I_2 = \frac{U}{sC_2R_sR_o + s^2CL_3R_s + s^2CL_1R_o + s^3CL_1L_3 + sL_1 + sL_3 + R_s + R_o}$$

$$\text{But} : y = i_2R_o$$

$$\therefore Y = I_2R_o$$

$$\therefore Y = \frac{UR_o}{sC_2R_sR_o + s^2CL_3R_s + s^2CL_1R_o + s^3CL_1L_3 + sL_1 + sL_3 + R_s + R_o}$$

$$\text{Since} : y = h * u$$

$$Y = HU$$

$$H = \frac{Y}{U}$$

$$H = \frac{R_o}{sC_2R_sR_o + s^2CL_3R_s + s^2CL_1R_o + s^3CL_1L_3 + sL_1 + sL_3 + R_s + R_o}$$

Since $L_1 = L_3 =$ L, $R_s = R_o =$ R, C

$$H = \frac{\frac{R}{CL^2}}{s^3 + \frac{2R}{L}s^2 + (\frac{2}{LC} + \frac{R^2}{L^2})s + \frac{2R}{L^2C}}$$

After substituting in component values and reducing in terms of ω_c

$$H(s) = \frac{\frac{\omega_c^3}{2}}{s^3 + 2\omega_c s^2 + 2\omega_c^2 s + \omega_c^3}$$

state variable technique

$$\begin{aligned}
\frac{di_1}{dt} &= a_{11}i_1 + a_{12}v_2 + a_{13}i_3 + b_{11}u \\
\frac{dv_2}{dt} &= a_{21}i_1 + a_{22}v_2 + a_{23}i_3 + b_{21}u \\
\frac{di_3}{dt} &= a_{31}i_1 + a_{32}v_2 + a_{33}i_3 + b_{31}u \\
y &= c_{11}i_1 + c_{12}v_2 + c_{13}i_3 + d_{11}u
\end{aligned}$$

$$\begin{aligned}
\frac{dx}{dt} &= [A]x + [B]u \\
\therefore sX &= [A]X + [B]U \\
\therefore (s[I]-[A])X &= [B]U \\
\therefore X &= (s[I]-[A])^{-1}[B]U \\
\text{and y} &= [C]x + [D]u \\
\therefore Y &= [C]X + [D]U \\
\therefore Y &= \frac{[C]adj(s[I]-[A])^T[B]U}{det(s[I]-[A])} + [D]U \\
\text{But H} = \frac{Y}{U} \therefore H &= \frac{[C]adj(s[I]-[A])^T[B]}{det(s[I]-[A])} + [D]
\end{aligned}$$

Where :

$$(s[I]-[A]) = \begin{bmatrix} s+\frac{R}{L} & \frac{1}{L} & 0 \\ \frac{-1}{C} & s & \frac{1}{C} \\ 0 & \frac{-1}{L} & s+\frac{R}{L} \end{bmatrix}, [C] = \begin{bmatrix} 0 & 0 & R_o \end{bmatrix}, [B] = \begin{bmatrix} \frac{1}{L_1} \\ 0 \\ 0 \end{bmatrix}, [D] = \begin{bmatrix} 0 \end{bmatrix}$$

$$\begin{aligned}
det(s[I]-[A]) &= s^3 + (\frac{R_o}{L_3} + \frac{R_s}{L_1})s^2 + (\frac{1}{L_3C_2} + \frac{1}{L_1C_2} + \frac{R_oR_s}{L_3L_1})s + \frac{R_o+R_s}{L_1L_3C_2} \\
\text{and } [C]adj(s[I]-[A])^T[B] &= \frac{R_o}{CL_1L_3} \\
\therefore H(s) &= \frac{\frac{R_o}{CL_1L_3}}{s^3 + (\frac{R_o}{L_3} + \frac{R_s}{L_1})s^2 + (\frac{1}{L_3C_2} + \frac{1}{L_1C_2} + \frac{R_oR_s}{L_3L_1})s + \frac{R_o+R_s}{L_1L_3C_2}}
\end{aligned}$$

After substituting in component values and reducing in terms of ω_c

$$H(s) = \frac{\frac{\omega_c^3}{2}}{s^3 + 2\omega_c s^2 + 2\omega_c^2 s + \omega_c^3}$$

It was very reassuring that both the matrix loop equation and state variable technique produced the same transfer function for their common circuit.

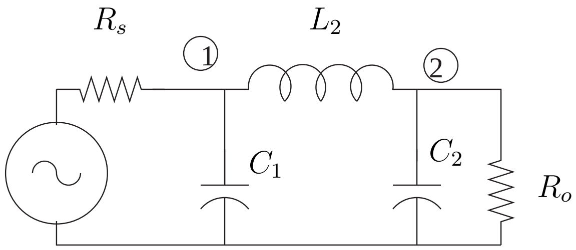

Figure 4: The "π" CLC circuit

Question 3

Matrix node equation

Node 1

$$
\begin{aligned}
\sum i = 0 &= i_{Rs} + i_{L2} + i_{C1} \\
0 &= \frac{v_{Rs}}{R_s} + C_1 \frac{dv}{dt} + \frac{1}{L_2} \int_0^t v d\tau + i(0) \\
0 &= \frac{u - v_1}{R_s} + C_1 \frac{d(0 - v_1)}{dt} + \frac{1}{L_2} \int_0^t (v_2 - v_1) d\tau + i(0) \\
0 &= \frac{\frac{du}{dt} - \frac{dv_1}{dt}}{R_s} - C_1 \frac{d^2(v_1)}{dt} + \frac{1}{L_2}(v_2 - v_1) \\
=> 0 &= \frac{s(U - V_1)}{R_s} - s^2 C_1 V_1 + \frac{1}{L_2}(V_2 - V_1) \text{ (Laplace)} \\
0 &= \frac{U - V_1}{R_s} - sC_1 V_1 + \frac{1}{sL_2}(V_2 - V_1) \\
U &= (1 + sC_1 R_s + \frac{R_s}{sL_2})V_1 - \frac{R_s}{sL_2} V_2
\end{aligned}
$$

Node 2

$$
\begin{aligned}
\sum i = 0 &= i_{L2} + i_{C2} + i_{Ro} \\
0 &= \frac{v_{Ro}}{R_o} + C_2 \frac{dv}{dt} + \frac{1}{L_2} \int_0^t v d\tau + i(0) \\
0 &= \frac{v_2}{R_o} + C_2 \frac{d(v_2)}{dt} - \frac{1}{L_2} \int_0^t (v_1 - v_2) d\tau - i(0) \\
0 &= \frac{\frac{dv_2}{dt}}{R_o} + C_2 \frac{d^2(v_2)}{dt} - \frac{1}{L_2}(v_1 - v_2) \\
=> 0 &= \frac{sV_2}{R_o} + s^2 C_2 V_2 - \frac{1}{L_2}(V_1 - V_2) \text{ (Laplace)} \\
0 &= \frac{V_2}{R_o} + sC_2 V_2 - \frac{1}{sL_2}(V_1 - V_2)
\end{aligned}
$$

$$0 = \frac{-1}{sL_2}V_1 + (\frac{1}{sL_2} + sC_3 + \frac{1}{R_o})V_2$$

$$\begin{bmatrix} (1 + sC_1R_s + \frac{R_s}{sL_2}) & \frac{-R_s}{sL_2} \\ \frac{-1}{sL_2} & (\frac{1}{sL_2} + sC_3 + \frac{1}{R_o}) \end{bmatrix} \begin{bmatrix} V_1 \\ V_2 \end{bmatrix} = \begin{bmatrix} U \\ 0 \end{bmatrix}$$

$$\begin{bmatrix} V_1 \\ V_2 \end{bmatrix} = \begin{bmatrix} (1 + sC_1R_s + \frac{R_s}{sL_2}) & \frac{-R_s}{sL_2} \\ \frac{-1}{sL_2} & (\frac{1}{sL_2} + sC_3 + \frac{1}{R_o}) \end{bmatrix}^{-1} \begin{bmatrix} U \\ 0 \end{bmatrix}$$

$$\text{But}: y = v_2$$

$$\therefore Y = V_2$$

$$\therefore Y = \frac{1}{det}\frac{U}{sL_2}$$

$$\text{where}: sL_2 \times det =$$

$$c_1R_sC_3L_2(s^3 + (\frac{1}{C_1R_s} + \frac{1}{C_3R_o})s^2 + (\frac{1}{C_1R_sC_3R_o} + \frac{1}{C_3L_2} + \frac{1}{C_1L_2})s + \frac{1}{R_oC_1C_3L_2} + \frac{1}{R_sC_1C_3L_2})$$

$$\text{But}: Y = HU$$

$$\therefore H = \frac{\frac{1}{c_1R_sC_3L_2}}{(s^3 + (\frac{1}{C_1R_s} + \frac{1}{C_3R_o})s^2 + (\frac{1}{C_1R_sC_3R_o} + \frac{1}{C_3L_2} + \frac{1}{C_1L_2})s + \frac{1}{R_oC_1C_3L_2} + \frac{1}{R_sC_1C_3L_2})}$$

After substituting in component values and reducing in terms of ω_c

$$H(s) = \frac{\frac{\omega_c^3}{2}}{s^3 + 2\omega_c s^2 + 2\omega_c^2 s + \omega_c^3}$$

state variable technique

$$\begin{aligned}\frac{di_1}{dt} &= a_{11}i_1 + a_{12}v_2 + a_{13}i_3 + b_{11}u \\ \frac{dv_2}{dt} &= a_{21}i_1 + a_{22}v_2 + a_{23}i_3 + b_{21}u \\ \frac{di_3}{dt} &= a_{31}i_1 + a_{32}v_2 + a_{33}i_3 + b_{31}u \\ y &= c_{11}i_1 + c_{12}v_2 + c_{13}i_3 + d_{11}u\end{aligned}$$

Identical algebra to that covered in Question 2 : state variable

$$\therefore H = \frac{[C]adj(s[I]-[A])^T[B]}{det(s[I]-[A])} + [D]$$

$$(s[I]-[A]) = \begin{bmatrix} s+\frac{1}{R_sC_1} & \frac{1}{C_1} & 0 \\ \frac{-1}{L_2} & s & \frac{1}{L_2} \\ 0 & \frac{-1}{C_3} & s+\frac{1}{RoC_3} \end{bmatrix}, [C] = \begin{bmatrix} 0 & 0 & 1 \end{bmatrix}, [B] = \begin{bmatrix} \frac{1}{R_sC_1} \\ 0 \\ 0 \end{bmatrix}, [D] = \begin{bmatrix} 0 \end{bmatrix}$$

$$det(s[I]-[A]) =$$

$$s^3+(\frac{1}{R_oC_1}+\frac{1}{R_sC_3})s^2+(\frac{1}{C_1L_2}+\frac{1}{C_3L_2}+\frac{1}{R_oR_sC_1C_3})s+\frac{1}{R_oR_s}+\frac{1}{R_sR_oC_1L_2}+\frac{1}{R_sR_oC_3L_2}$$

$$\text{and } [C]adj(s[I]-[A])^T[B] = \frac{1}{R_sC_1L_2C_3}$$

$$\therefore H(s) =$$

$$\frac{\frac{1}{R_sC_1L_2C_3}}{s^3+(\frac{1}{R_oC_1}+\frac{1}{R_sC_3})s^2+(\frac{1}{C_1L_2}+\frac{1}{C_3L_2}+\frac{1}{R_oR_sC_1C_3})s+\frac{1}{R_oR_s}+\frac{1}{R_sR_oC_1L_2}+\frac{1}{R_sR_oC_3L_2}}$$

After substituting in component values and reducing in terms of ω_c

$$H(s) = \frac{\frac{\omega_c^3}{2}}{s^3+2\omega_c s^2+2\omega_c^2 s+\omega_c^3}$$

Again the separate derivations converged on the same transfer function, and corroborated the earlier transfer function garnered from the "T" configuration topology. This consistency verified the inherent characteristics of the filter which are independent of the topology we choose to adopt.

Question 4

Characteristic polynomial : $s^3 + s^2 2\omega_c + s2\omega_c^2 + \omega_c^3$
System differential equation : $\frac{d^3y}{dt} + 2\omega_c\frac{d^2y}{dt} + 2\omega_c^2\frac{dy}{dt} + \omega_c^3 y = \frac{\omega_c^3}{2}U$

Question 5

There are no zeros since there are no s terms in the numerator. We need to discover the poles of the transfer function, so we simply factorise the denominator.

$$\frac{1}{s^3 + s^2 2\omega_c + s2\omega_c^2 + \omega_c^3}$$
$$\frac{1}{(s+\omega_c)(s^2 + \omega_c s + \omega_c^2)}$$
$$\frac{1}{(s+\omega_c)(s + \frac{\omega_c}{2} + j\frac{\sqrt{3}}{2}\omega_c)(s + \frac{\omega_c}{2} - j\frac{\sqrt{3}}{2}\omega_c)}$$

$$\begin{aligned} \therefore \text{eigenfrequencies : } s &= -\omega_c \\ \text{or} & \\ s &= -\frac{\omega_c}{2} + j\frac{\sqrt{3}}{2}\omega_c \\ \text{or} & \\ s &= -\frac{\omega_c}{2} - j\frac{\sqrt{3}}{2}\omega_c \end{aligned}$$

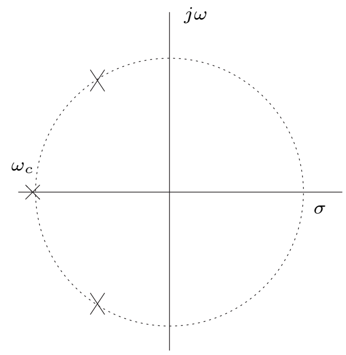

Figure 5: Pole Zero diagram

Since the poles are all on the left hand side of the imaginary axis, we know from our notes that the filter is stable.

Question 6

$$
\begin{aligned}
H(s) &= \frac{\frac{\omega_c^3}{2}}{s^3 + 2\omega_c s^2 + 2\omega_c^2 s + \omega_c^3} \\
H(s) &= \frac{\frac{\omega_c^3}{2}}{(s+\omega_c)(s+\frac{\omega_c}{2}+j\frac{\sqrt{3}}{2}\omega_c)(s+\frac{\omega_c}{2}-j\frac{\sqrt{3}}{2}\omega_c)} \\
H(j\omega) &= \frac{\frac{\omega_c^3}{2}}{(j\omega+\omega_c)(j\omega+\frac{\omega_c}{2}-\frac{\sqrt{3}}{2}j\omega_c)(j\omega+\frac{\omega_c}{2}+\frac{\sqrt{3}}{2}j\omega_c)}
\end{aligned}
$$

Magnitude is given by :

$$
|H(j\omega)| = \frac{|\frac{\omega_c^3}{2}|}{|(j\omega+\omega_c)||(j\omega+\frac{\omega_c}{2}-\frac{\sqrt{3}}{2}j\omega_c)||(j\omega+\frac{\omega_c}{2}+\frac{\sqrt{3}}{2}j\omega_c)|}
$$

Phase is given by :

$$
\angle H(j\omega) = -\angle(j\omega+\omega_c) - \angle(j\omega+\frac{\omega_c}{2}-\frac{\sqrt{3}}{2}j\omega_c) - \angle(j\omega+\frac{\omega_c}{2}+\frac{\sqrt{3}}{2}j\omega_c)
$$

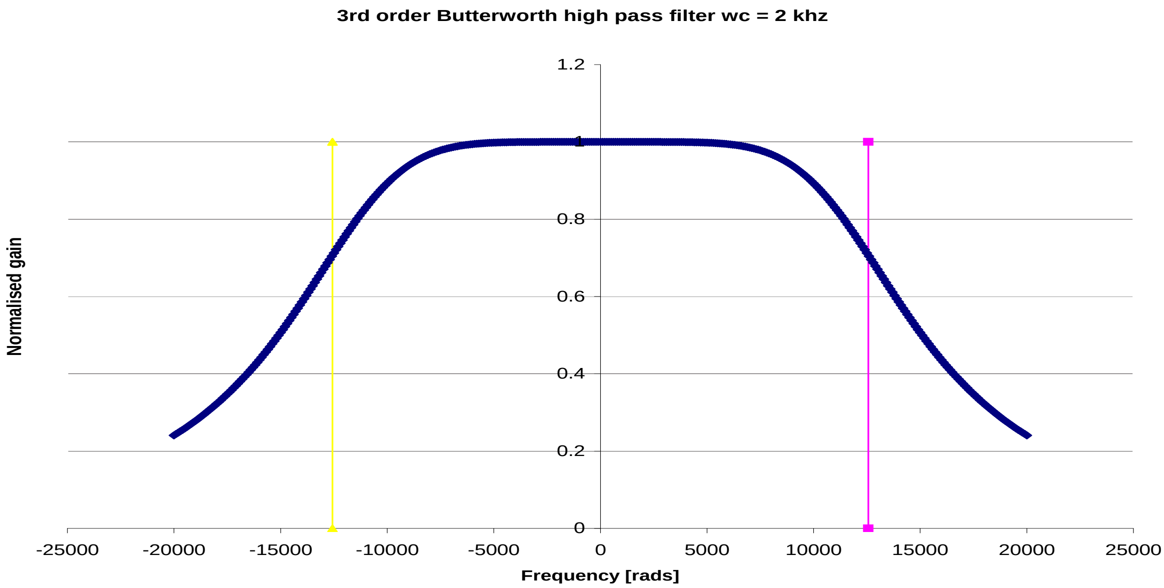

Figure 6: excel : Normalised gain vs frequency

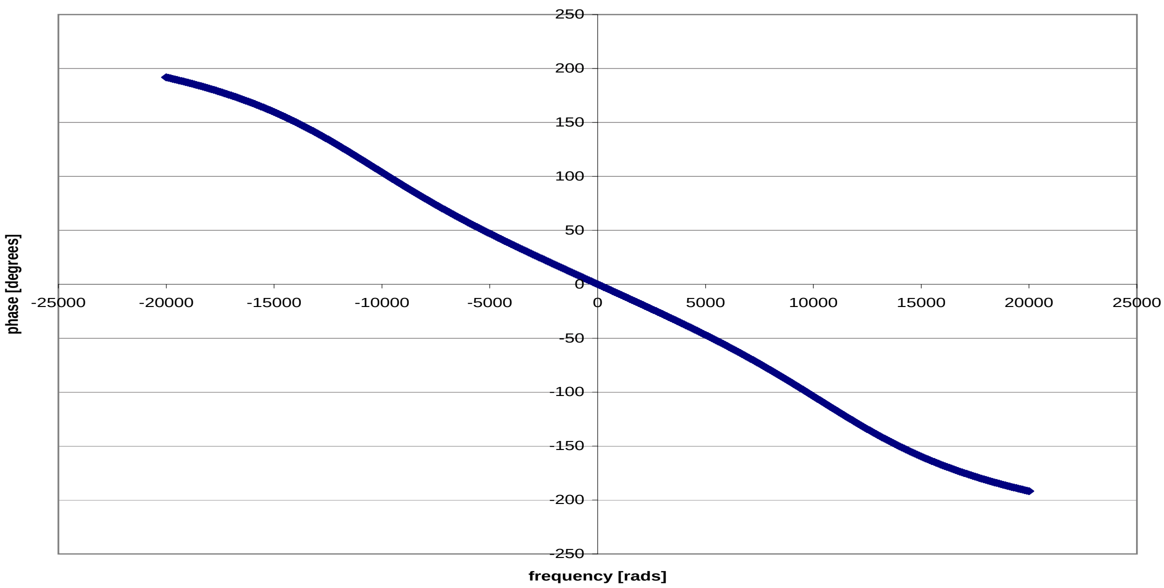

Figure 7: excel : phase vs frequency

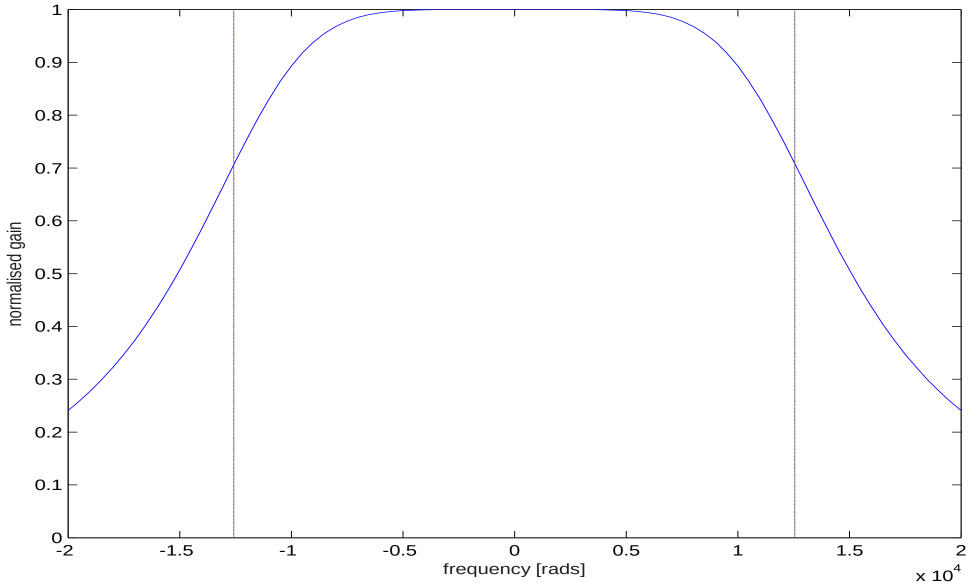

Figure 8: matlab : gain vs frequency

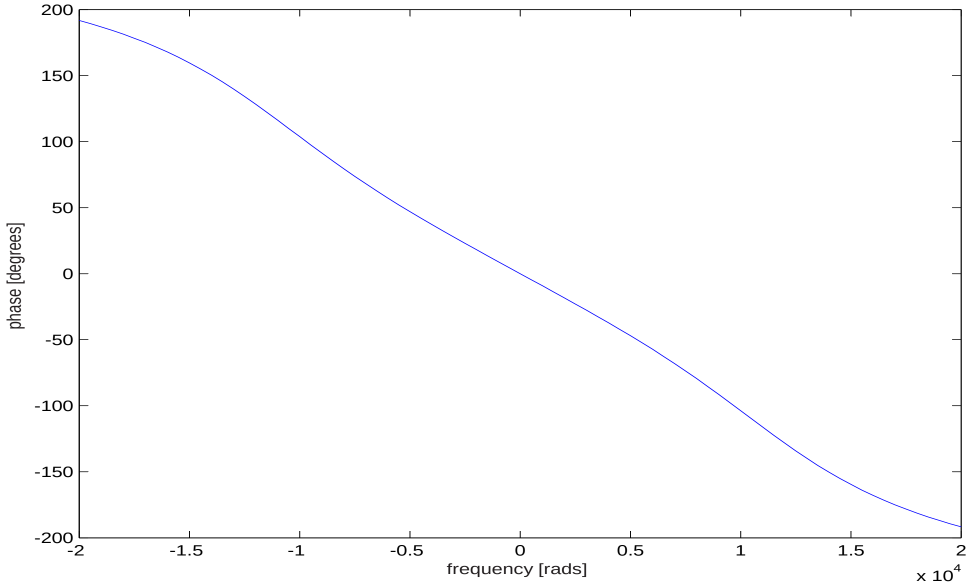

Figure 9: matlab : phase vs frequency

These graphs, which were derived independently in excel and matlab, are consistent with each other and show the transfer function behaving as expected, with the flat passband characterstic of a Butterworth filter. The filter allows low frequencies through, and attenuates the amplitude of the input signal by $\sqrt{2}$ at the cutoff frequency. ($\omega_c \approx 12000$ rads)

Question 7

Looking at the pole zero diagram, we can imagine a third dimension, representing gain, stemming out of the page with the poles rising off to infinity and stretching the surrounding area upwards. Looking at the imaginary axis, we can see the angular frequency running off to infinity in both directions. At the origin the gain is a maximum, with all three poles pulling up the surrounding area. As the angular frequency increases away in both directions the gain diminishes as the vector distance from all three poles steadily increases. The flat passband evident in the gain vs frequency graph, is conveyed in the varying real/imaginary components of the poles. The completely real pole has the largest impact on gain, with the conjugate imaginary poles constructively adding their gain as the gain from the real pole rolls off.

Question 8

$$\frac{\alpha}{(s+\omega_c)(s+\frac{\omega_c}{2}+j\frac{\sqrt{3}}{2}\omega_c)(s+\frac{\omega_c}{2}-j\frac{\sqrt{3}}{2}\omega_c)} = \frac{K_1}{(s+\omega_c)} + \frac{K_2}{(s+\frac{\omega_c}{2}+j\frac{\sqrt{3}}{2}\omega_c)} + \frac{K_3}{(s+\frac{\omega_c}{2}-j\frac{\sqrt{3}}{2}\omega_c)}$$

$$\therefore \frac{\frac{\omega_c^3}{2}}{(s+\omega_c)(s+\frac{\omega_c}{2}+j\frac{\sqrt{3}}{2}\omega_c)(s+\frac{\omega_c}{2}-j\frac{\sqrt{3}}{2}\omega_c)} = \frac{K_1}{(s+\omega_c)} + \frac{K_2}{(s+\frac{\omega_c}{2}+j\frac{\sqrt{3}}{2}\omega_c)} + \frac{K_3}{(s+\frac{\omega_c}{2}-j\frac{\sqrt{3}}{2}\omega_c)}$$

Question 8	wc		12566.37061
h	=		100
wc/2	=		6283.185307
root(3)/2*jwc	=	10882.7961854053i	
p1	p2	p3	
wc	-wc/2 - j(root(3)/2*wc)	-wc/2 + j(root(3)/2*wc)	
-12566.37061	-6283.18530717959-10882.7961854053i	-6283.18530717959+10882.7961854053i	
	alpha		9.92201E+11
	residues		
k1	6283.18530717961		
k2	-3141.5926535898+1813.79936423422i		
k3	-3141.5926535898-1813.79936423422i		

Figure 10: Excel calculated residues

```
4/23/05 2:10 PM              MATLAB Command Window                    1 of 1

alpha =

  9.9220e+011


K1 =

  6.2832e+003


K2 =

 -3.1416e+003 +1.8138e+003i


K3 =

 -3.1416e+003 -1.8138e+003i
```

Figure 11: Matlab calculated residues

Question 9

The Laplace transform of
$\frac{\alpha}{(s+\omega_c)(s+\frac{\omega_c}{2}+j\frac{\sqrt{3}}{2}\omega_c)(s+\frac{\omega_c}{2}-j\frac{\sqrt{3}}{2}\omega_c)} \approx K_1e^{p_1t}+K_2e^{p_2t}+K_3e^{p_3t} = h(t)$

Where :
K_1 = 6283.18530717961
K_2 = -3141.5926535898+1813.79936423422i
K_3 = -3141.5926535898-1813.79936423422i
p_1 = -12566.37061
p_2 = -6283.18530717959-10882.7961854053i
p_3 = -6283.18530717959+10882.7961854053i

$$
\begin{aligned}
\therefore h(t) &= K_1e^{p_1t}+K_2e^{p_2t}+K_3e^{p_3t} \\
h(t) &= K_1e^{12566.37061t}+|K|e^{-6283.18530717959t}(e^{i\angle K_2}e^{-i10882.7961854053t}+e^{i\angle K_3}e^{i10882.7961854053t}) \\
\text{Since } \angle K_2 &= \angle K_3 \text{ (Conjugate pair)} \\
h(t) &= K_1e^{12566.37061t}+|K|e^{-6283.18530717959t}(e^{-i(\angle K_3+10882.7961854053t)}+e^{i(\angle K_3+10882.7961854053t)}) \\
h(t) &= K_1e^{12566.37061t}+2|K|e^{-6283.18530717959t}cos(\angle K_3+10882.7961854053t)
\end{aligned}
$$

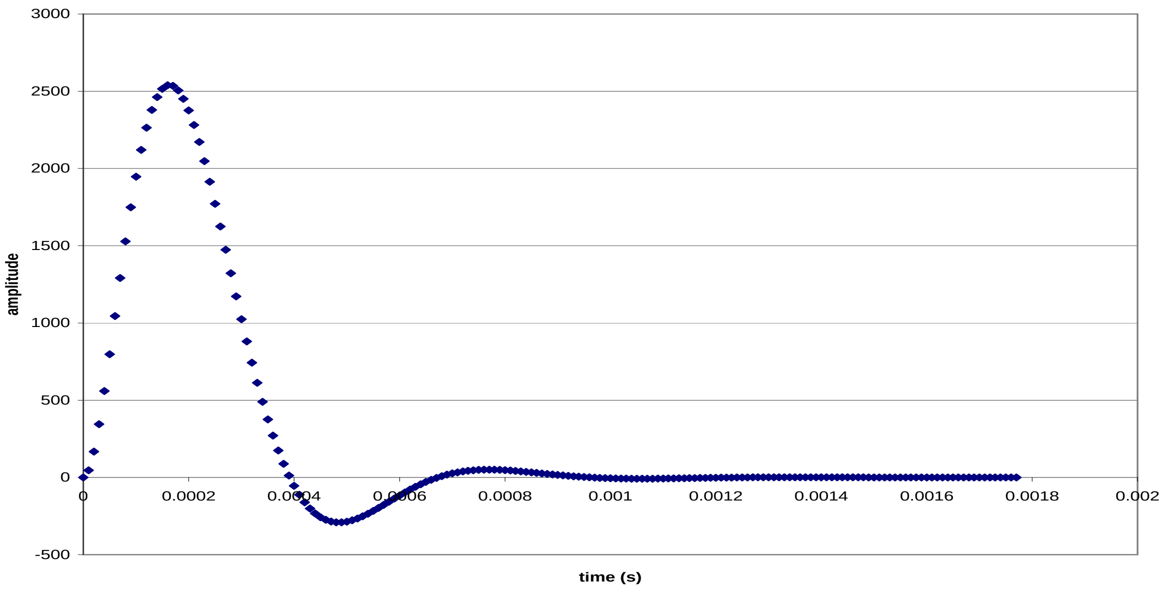

Figure 12: Excel impulse response

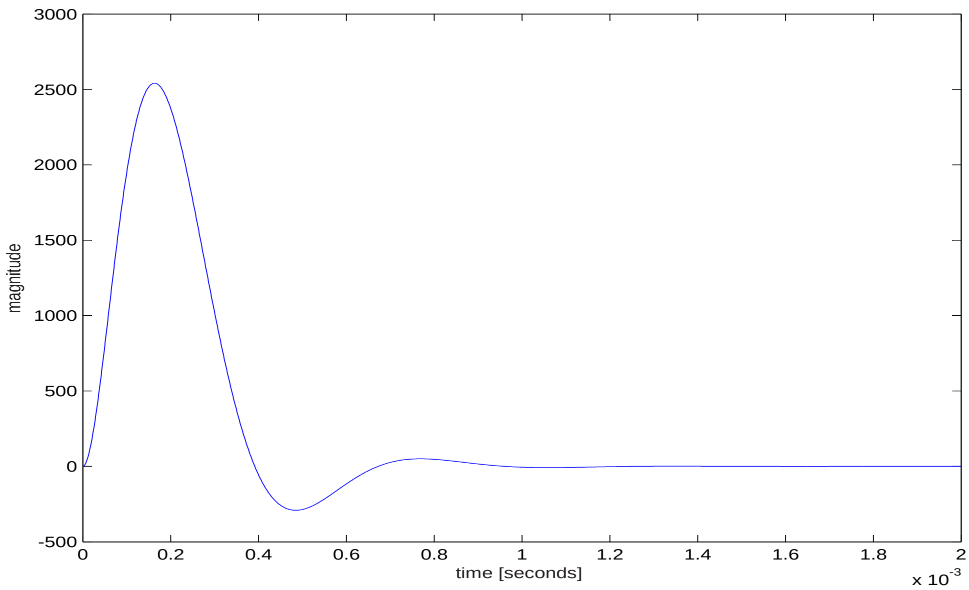

Figure 13: MatLab impulse response

Question 10

Using the the bilinear transform within Matlab :
$\mathcal{P}_i = \frac{1+\frac{T}{2}P_i}{1-\frac{T}{2}P_i}$

$f_{sample}[hz]$	$\mathcal{P}_1$	$\mathcal{P}_2$	$\mathcal{P}_3$
48000	0.7685	0.8561 - 0.1975i	0.8561 + 0.1975i
8000	0.1202	0.1595 - 0.5663i	0.1595 + 0.5663i

Table 1: Matlab generated poles for the digital filters

This bilinear transformation shifts the frequency response of the resulting filters. The higher the sampling frequency, the milder the resulting shift in frequency response. The filter with $f_{sample} = 48$kHz therefore basically retains its initial frequency characteristics, while the filter with $f_{sample} = 8$kHz has its f_c dropped to 1700Hz.

Question 11

$$
\begin{aligned}
H(z) &= \kappa \frac{(1+z^{-1})^{N-M}\prod_{i=1}^{M}(1-Z_i z^{-1})}{\prod_{i=1}^{N}(1-\mathcal{P}_i z^{-1})} \\
& \text{Where there are M = 0 zeros and N = 3 poles} \\
\therefore H(z) &= \kappa \frac{(1+z^{-1})^{3}}{\prod_{i=1}^{3}(1-\mathcal{P}_i z^{-1})} \\
& \text{Where the values of the poles are given in table 1 (above) and} \\
\kappa &= K(\frac{T}{2})^{N-M}\frac{\prod_{i=1}^{M}(1-\frac{T}{2}Z_i)}{\prod_{i=1}^{N}(1-\frac{T}{2}P_i)} \\
\kappa &= \frac{\omega_c^3}{2}(\frac{T}{2})^3\frac{1}{\prod_{i=1}^{3}(1-\frac{T}{2}P_i)}
\end{aligned}
$$

$frequency$	κ
8000	0.0565
48000	0.000864

Table 2: κ values

for $f_{sample} = 48000\text{Hz}$

$$H(z) = \kappa_{48000} \frac{(1+z^{-1})^3}{(1-0.7685z^{-1})(1-(0.8561-0.1975i)z^{-1})(1-(0.8561+0.1975i)z^{-1})}$$

for $f_{sample} = 8000\text{Hz}$

$$H(z) = \kappa_{8000} \frac{(1+z^{-1})^3}{(1-0.1202z^{-1})(1-(0.1595-0.5663i)z^{-1})(1-(0.1595+0.5663i)z^{-1})}$$

Question 12

There are three zeros at -1, divulged from the numerator term. The denominator reveals three poles, demarcated by Xes on the graph

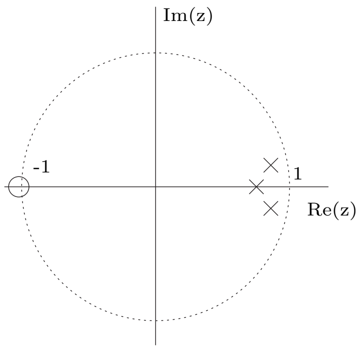

Figure 14: 48000 Hz filter Pole Zero diagram

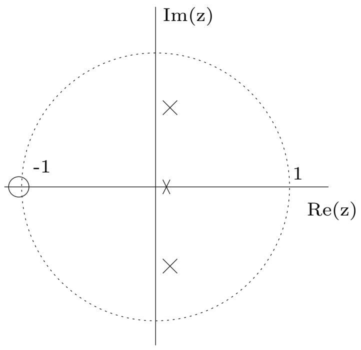

Figure 15: 8000 Hz filter Pole Zero diagram

Question 13

Similarly to question 6

Magnitude :

$$|H(z)| = \kappa \frac{|(1+z^{-1})|^3}{|(1-\mathcal{P}_1 z^{-1})||(1-\mathcal{P}_2 z^{-1})||(1-\mathcal{P}_3 z^{-1})|}$$

Where κ is taken from table 2 and $\mathcal{P}$ values are taken from table 1

Phase :

$$\angle H(z) = \Sigma\angle(zeros) - \Sigma\angle(poles)$$

$$\angle H(z) = 3 \times \angle(1+z^{-1}) - \angle(1-\mathcal{P}_1 z^{-1}) - \angle(1-\mathcal{P}_2 z^{-1}) - \angle(1-\mathcal{P}_3 z^{-1})$$

Both Matlab and excel were used in order to establish corroborative evidence for the frequency response of the filter. I felt this was necessary since the shifting inherent in the bilinear transform was not immediate obvious, and I was initially concerned with my results.

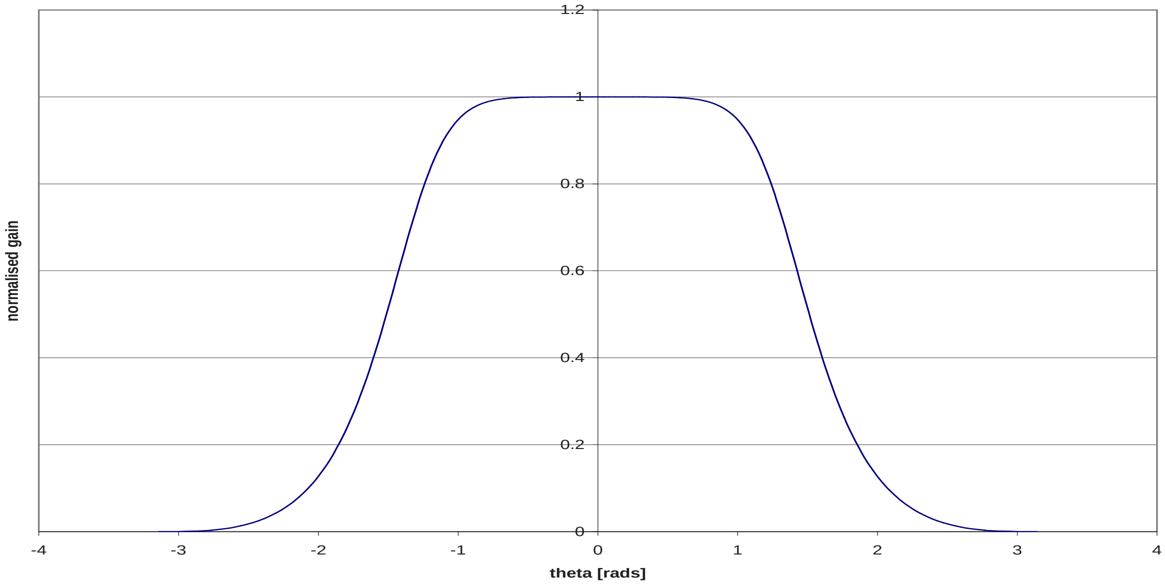

Figure 16: Excel: 8000 Hz digital filter normalised gain

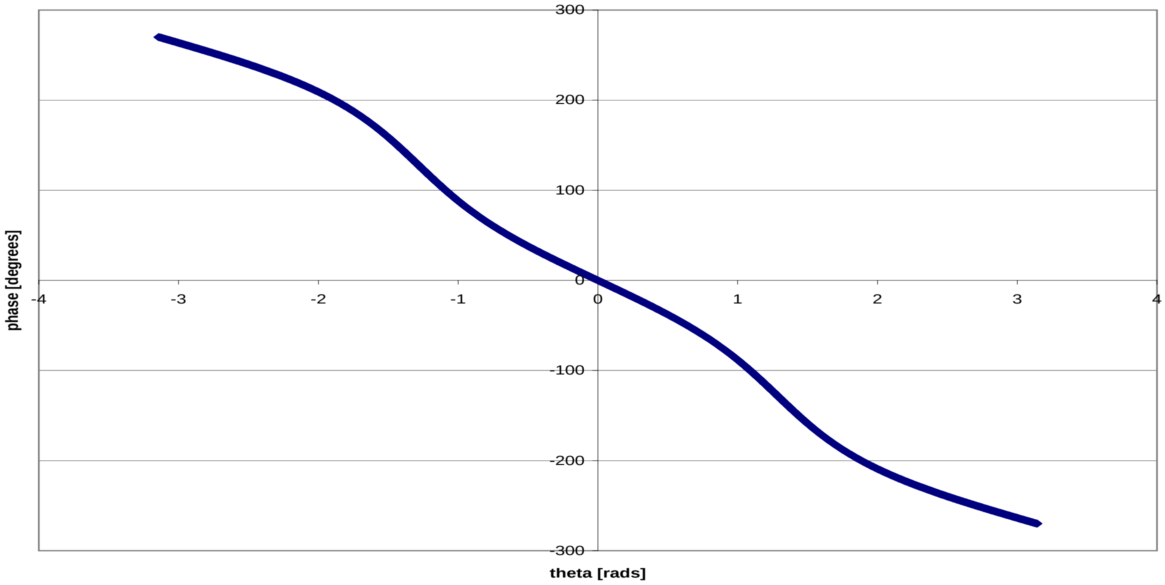

Figure 17: Excel: 8000 Hz digital filter phase response

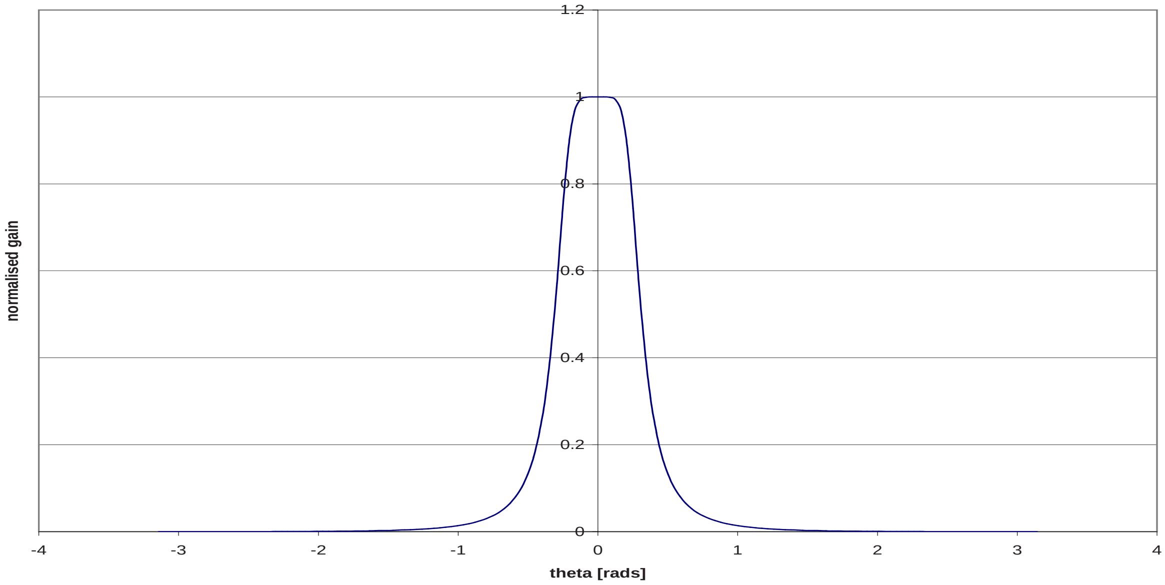

Figure 18: Excel: 48000 Hz digital filter normalised gain

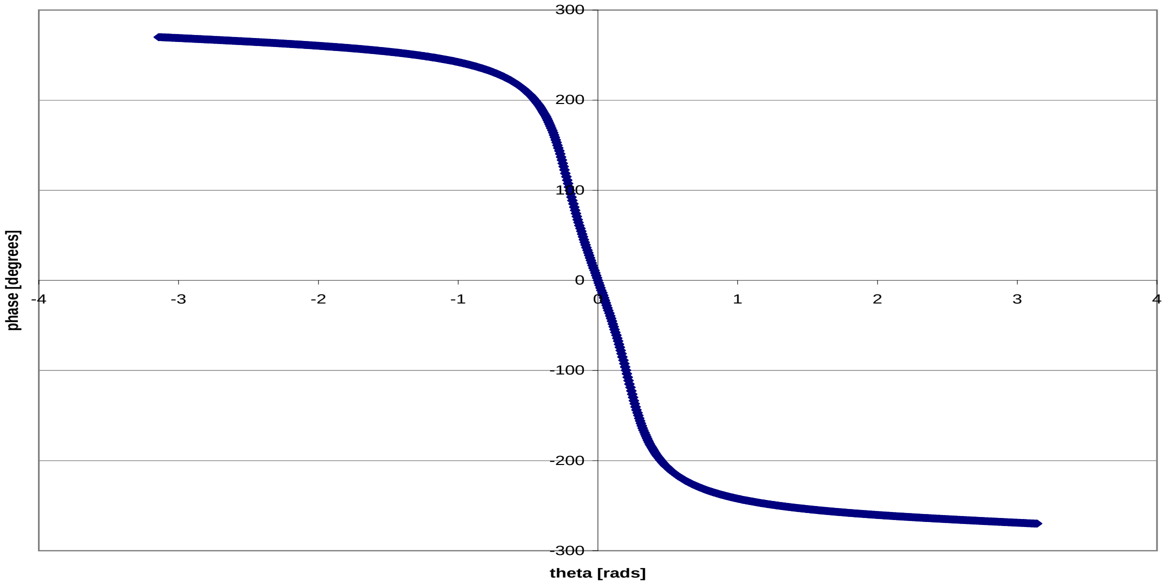

Figure 19: Excel: 48000 Hz digital filter phase response

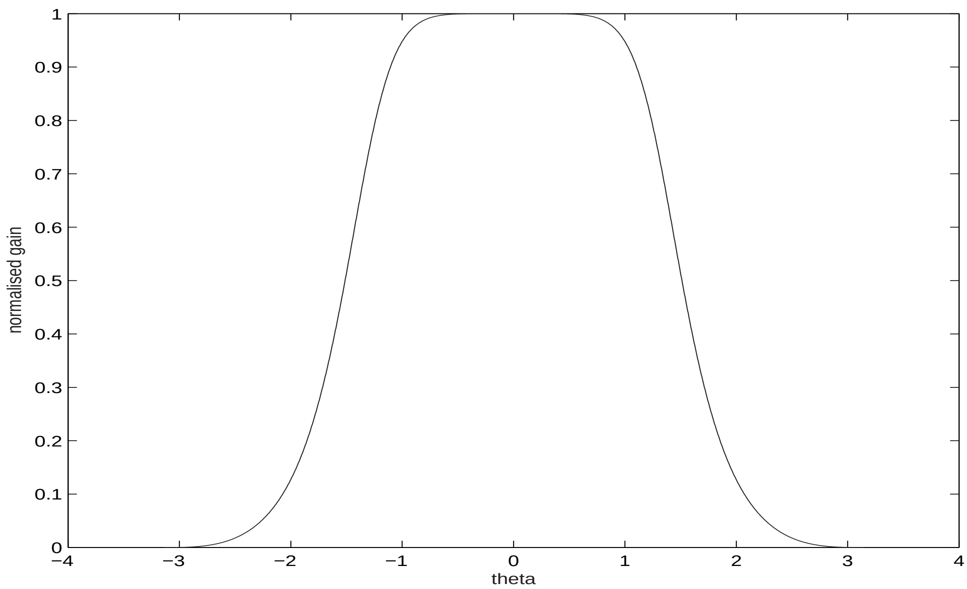

Figure 20: Matlab : 8000 Hz digital filter normalised gain

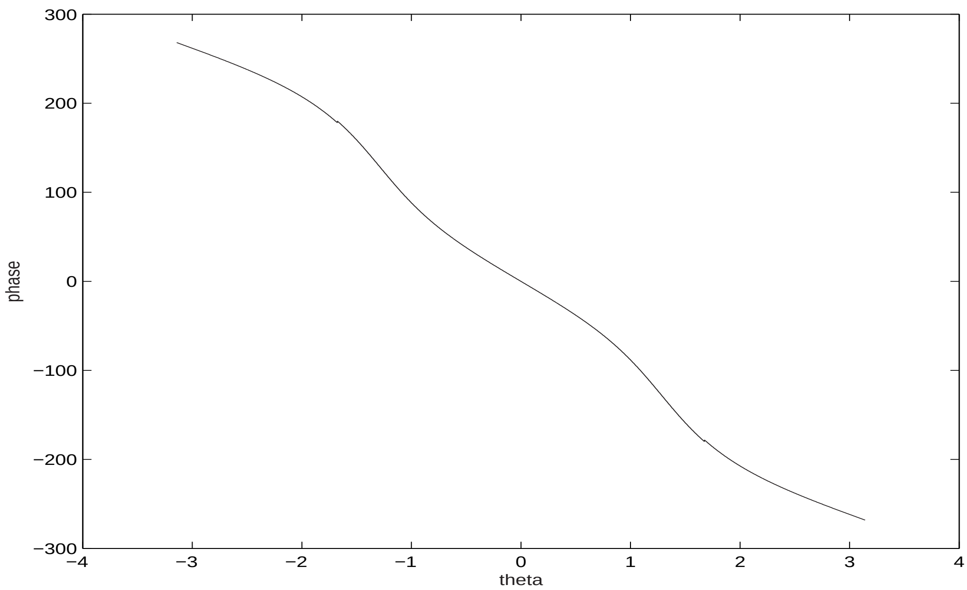

Figure 21: Matlab : 8000 Hz digital filter phase response

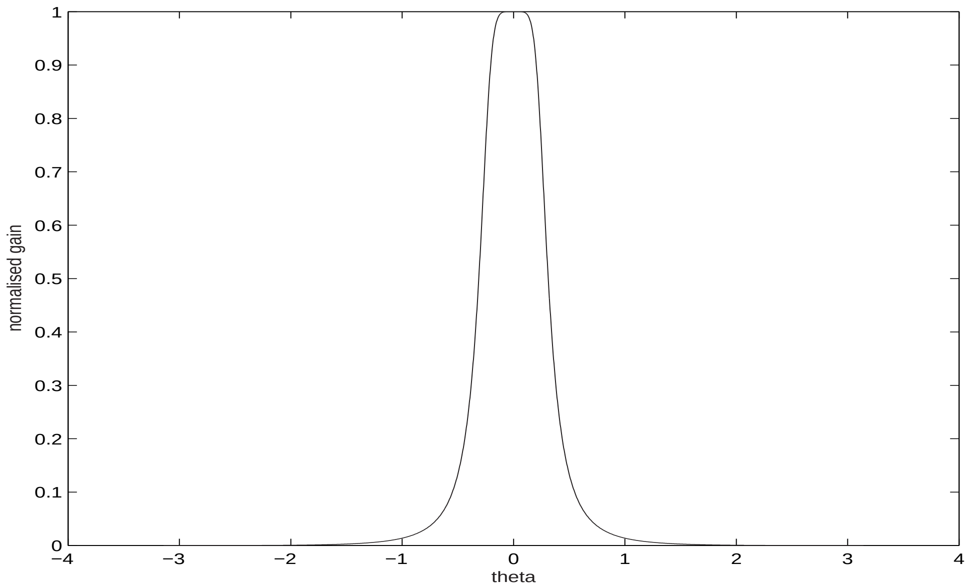

Figure 22: Matlab : 48000 Hz digital filter normalised gain

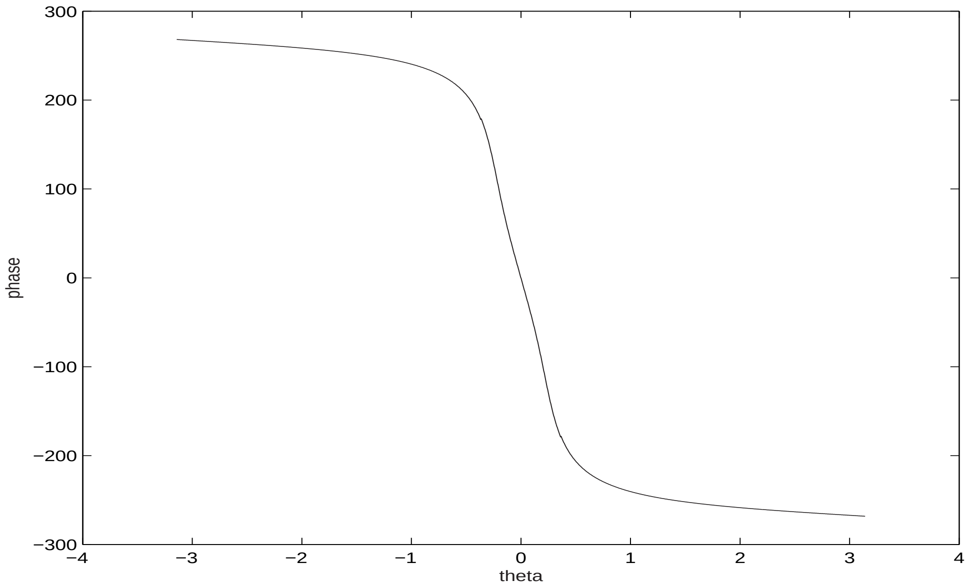

Figure 23: Matlab : 48000 Hz digital filter phase response

Question 14

$$
\begin{aligned}
H(z) &= \kappa \frac{(1+z^{-1})^3}{(1-\mathcal{P}_1 z^{-1})(1-\mathcal{P}_2 z^{-1})(1-\mathcal{P}_3 z^{-1})} \\
\text{But :} & \quad H(z) = \frac{Y(z)}{X(z)} \\
\therefore \frac{Y(z)}{X(z)} &= \kappa \frac{(1+z^{-1})^3}{(1-\mathcal{P}_1 z^{-1})(1-\mathcal{P}_2 z^{-1})(1-\mathcal{P}_3 z^{-1})}
\end{aligned}
$$

$$
Y(z) \times (1-\mathcal{P}_1 z^{-1})(1-\mathcal{P}_2 z^{-1})(1-\mathcal{P}_3 z^{-1}) = X(z) \times \kappa(1+z^{-1})^3
$$

$$
Y(z) \times (1-\mathcal{P}_1 z^{-1} - \mathcal{P}_2 z^{-1} - \mathcal{P}_3 z^{-1} + \mathcal{P}_1\mathcal{P}_2 z^{-2} + \mathcal{P}_2\mathcal{P}_3 z^{-2} + \mathcal{P}_1\mathcal{P}_3 z^{-2} - \mathcal{P}_1\mathcal{P}_2\mathcal{P}_3 z^{-3}) =
$$

$$
X(z) \times \kappa(1+3z^{-1}+3z^{-2}+z^{-3})
$$

Using the inverse Z transform properties given on pg. 25 of the digital section

$$
y_n - \mathcal{P}_1 y_{n-1} - \mathcal{P}_2 y_{n-1} - \mathcal{P}_3 y_{n-1} + \mathcal{P}_1\mathcal{P}_2 y_{n-2} + \mathcal{P}_2\mathcal{P}_3 y_{n-2} + \mathcal{P}_1\mathcal{P}_3 y_{n-2} - \mathcal{P}_1\mathcal{P}_2\mathcal{P}_3 y_{n-3}) =
$$

$$
\kappa(x_n + 3x_{n-1} + 3x_{n-2} + x_{n-3})
$$

$$
\begin{aligned}
y_n &= (\mathcal{P}_1+\mathcal{P}_2+\mathcal{P}_3) y_{n-1} - (\mathcal{P}_1\mathcal{P}_2+\mathcal{P}_2\mathcal{P}_3+\mathcal{P}_1\mathcal{P}_3) y_{n-2} + \mathcal{P}_1\mathcal{P}_2\mathcal{P}_3 y_{n-3} + \kappa(x_n + 3x_{n-1} + 3x_{n-2} + x_{n-3}) \\
y_n &= \alpha y_{n-1} - \beta y_{n-2} + \gamma y_{n-3} + \kappa(x_n + 3x_{n-1} + 3x_{n-2} + x_{n-3})
\end{aligned}
$$

This recurrence relation is common to both filters, with the coefficients of the terms assuming different values depending on the sampling frequency.

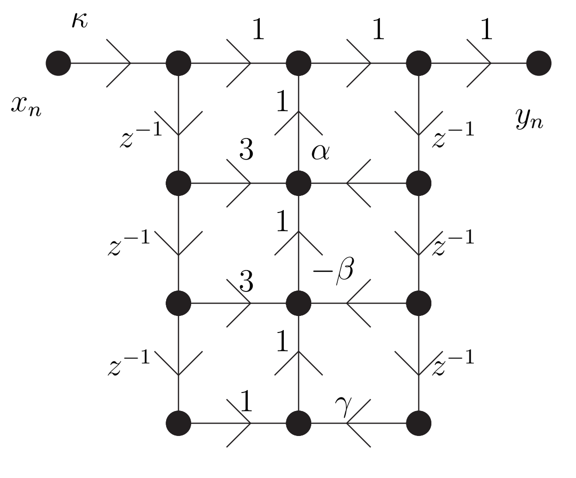

Figure 24: Signal flow diagram for both filters

The following coefficients were calculated in Matlab :

$f_{sample}[Hz]$	α	β	γ
8000	0.4392	0.3845	0.0416
48000	2.4808	2.0878	0.5933

Table 3: Matlab generated values for α,β and γ

Question 15

The unit sample responses of both digital filters corresponded strongly to the original impulse response calculated for the analogue filter, with the impulse response being clearly recognisable. The lower the initial sampling frequency, the faster the emergence of the recognisable response was when observing the discrete impulse response.

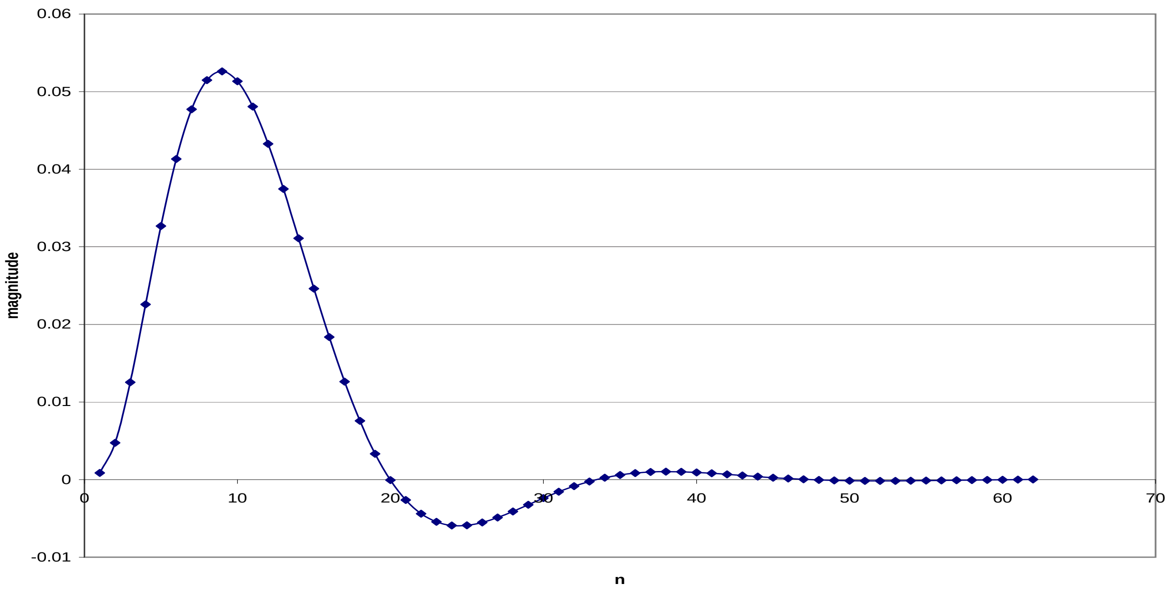

Figure 25: Matlab : 48000 Hz filter impulse response

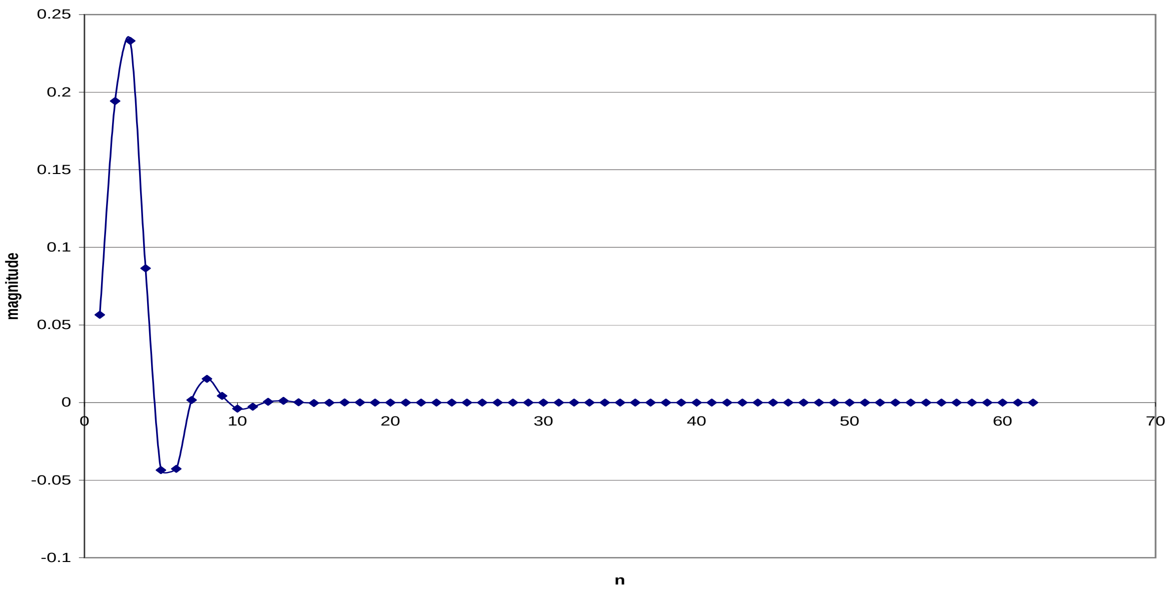

Figure 26: Matlab : 8000 Hz filter impulse response

Question 16

In designing an ideal low pass filter, we want a top-hat function in the frequency domain, ranging from $-\omega_c$ to ω_c

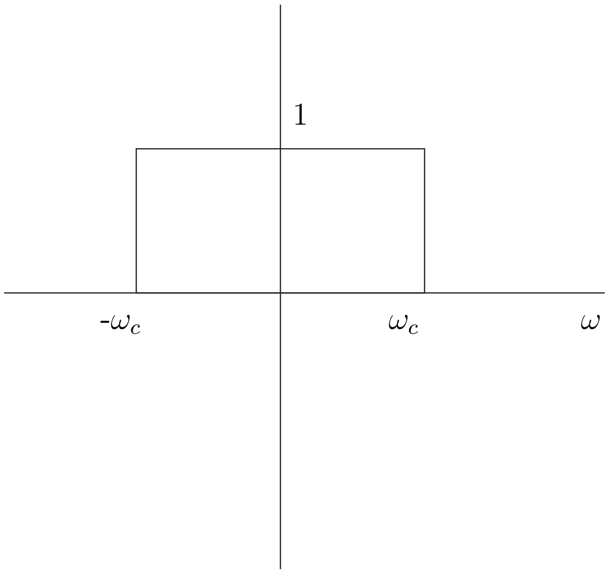

Figure 27: Ideal low pass filter frequency response

This transforms, via the inverse Fourier transform, into a sinc function in the time domain. We sample the signal at 41 different points in order to discover the magnitude of the signal at that point and the sampled impulse response can subsequently be digitally recreated by summing Dirac functions multiplied by these magnitudes.

The function is non-causal, so it must be shifted in the positive direction, and incomplete since the sinc function continues on to infinity in reality and we have discarded all the unsampled points. This impacts on the accuracy of recreation, and there are many different windowing methods devoted to easing this cut-off point.

As is clearly seen from graph 29, the different windowing functions attenuate the function to differing degrees and in different ways, as it approaches its cutoff frequency.

Our coefficients $(a_i)$are calculated by multiplying the shifted magnitudes of the sampled points by an appropriate windowing coefficient.

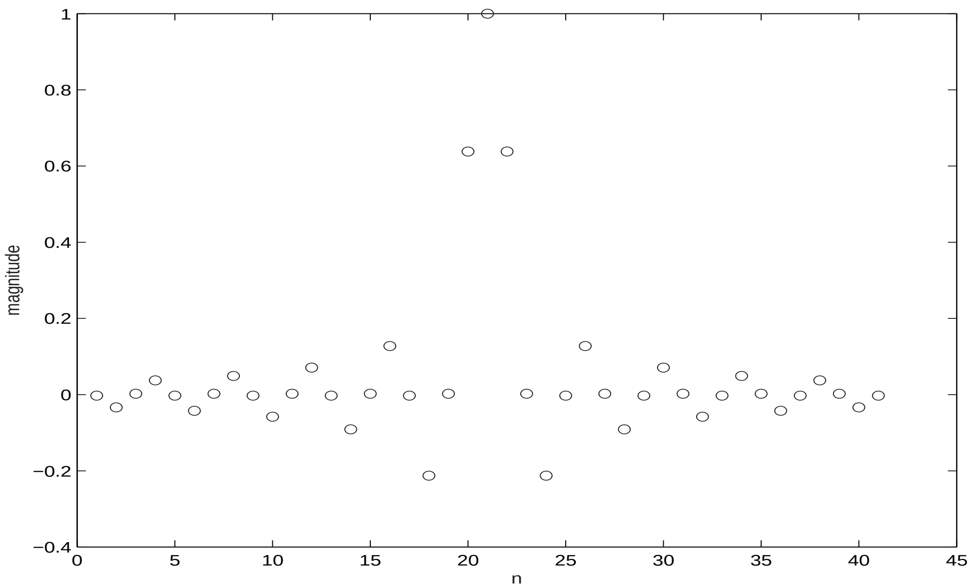

Figure 28: Recreated impulse response

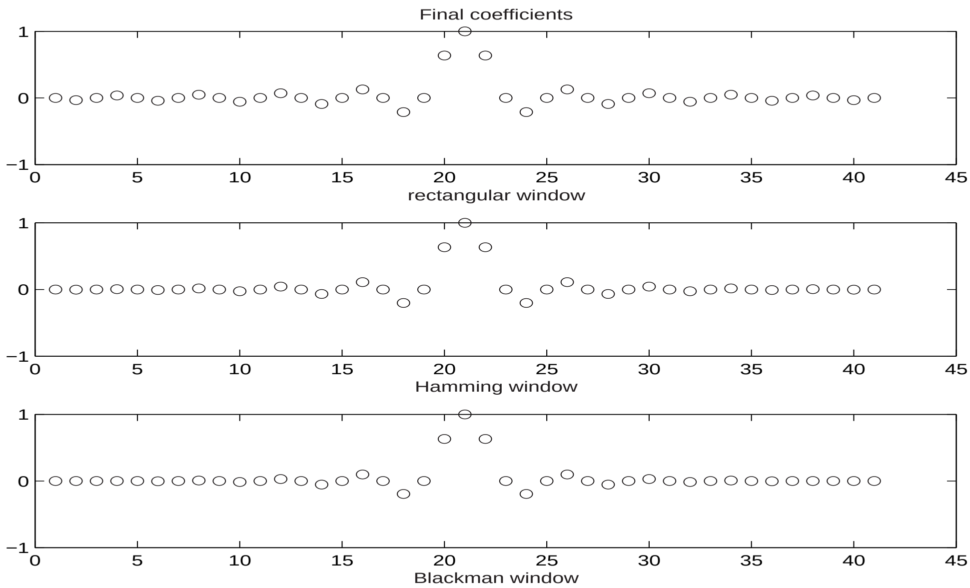

Figure 29: Different windowing methods

no	Rectangular	Hamming	Blackman
1	0	0	0
2	-0.0335	-0.0029	-0.0001
3	0	0	0
4	0.0374	0.0049	0.0008
5	0	0	0
6	-0.0424	-0.0091	-0.0028
7	0	0	0
8	0.049	0.0162	0.0071
9	0	0	0
10	-0.0579	-0.0271	-0.0154
11	0	0	0
12	0.0707	0.0433	0.0299
13	0	0	0
14	-0.0909	-0.0681	-0.0546
15	0	0	0
16	0.1273	0.1102	0.0985
17	0	0	0
18	-0.2122	-0.2016	-0.1936
19	0	0	0
20	0.6366	0.633	0.6302
21	1	1	1
22	0.6366	0.633	0.6302
23	0	0	0
24	-0.2122	-0.2016	-0.1936
25	0	0	0
26	0.1273	0.1102	0.0985
27	0	0	0
28	-0.0909	-0.0681	-0.0546
29	0	0	0
30	0.0707	0.0433	0.0299
31	0	0	0
32	-0.0579	-0.0271	-0.0154
33	0	0	0
34	0.049	0.0162	0.0071
35	0	0	0
36	-0.0424	-0.0091	-0.0028
37	0	0	0
38	0.0374	0.0049	0.0008
39	0	0	0
40	-0.0335	-0.0029	-0.0001
41	0	0	0

Table 4: Table of coefficients

Question 17

The recreated signal is therefore represented by :

$$
\begin{aligned}
h(n) &= \Sigma_{i=0}^{40} a_i \delta(n-i) \\
& \quad \text{The recurrence relation is there given by :} \\
y(n) &= h(n) * x(n) \\
y(n) &= \Sigma_{i=0}^{40} a_i \delta(n-i) * x(n) \\
y(n) &= \Sigma_{i=0}^{40} a_i x(n-i) (\text{unit impulse convolution})
\end{aligned}
$$

The transfer function can be deduced as :

$$
\begin{aligned}
y(n) &= \Sigma_{i=0}^{40} a_i x(n-i) \\
Y(z) &= \Sigma_{i=0}^{40} a_i X(z) z^{-i} (\text{Z transform}) \\
\frac{Y(z)}{X(z)} &= \Sigma_{i=0}^{40} a_i z^{-i} \\
\therefore H(z) &= \Sigma_{i=0}^{40} a_i z^{-i}
\end{aligned}
$$

Question 18

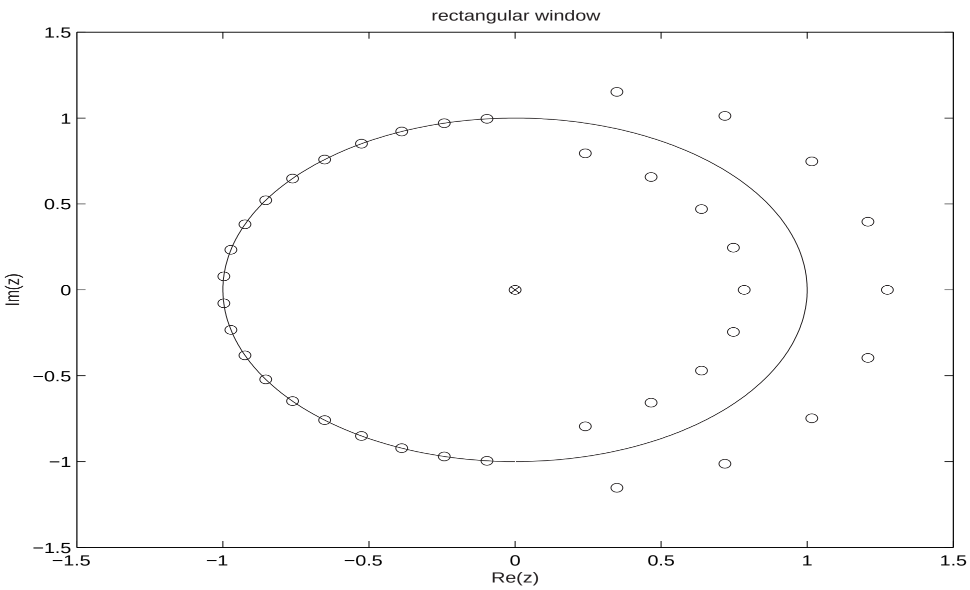

Figure 30: Rectangular window, pole zero diagram

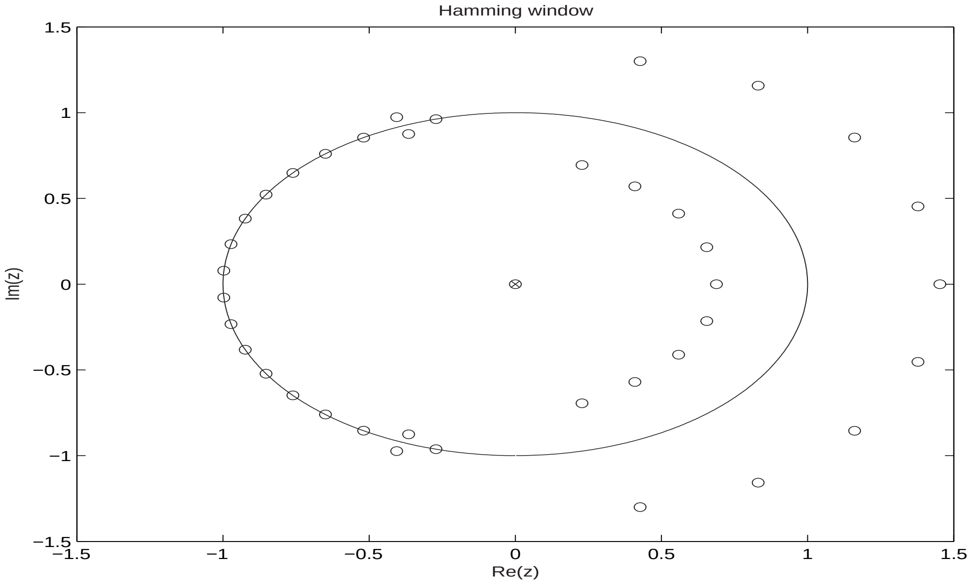

Figure 31: Hamming window, pole zero diagram

For some reason unbeknownst to me, the matlab roots function malfunctioned at 2000 kHz, leaving me with a severely unsatisfactory Blackman's window pole zero diagram. At 1995 kHz, the function stabilised, and gave me a pole zero diagram that was more readily believable in the context of the other plots.

There are three poles in each pole zero diagram, though they are clustered at the origin of each of the respective pole zero diagrams.

The zeros radiating beyond the unit circle were a point of some concern, before it was revealed that the location of the zeros was unrestricted, and that the presence of the poles within the unit circle was the only point of concern regarding filter stability.

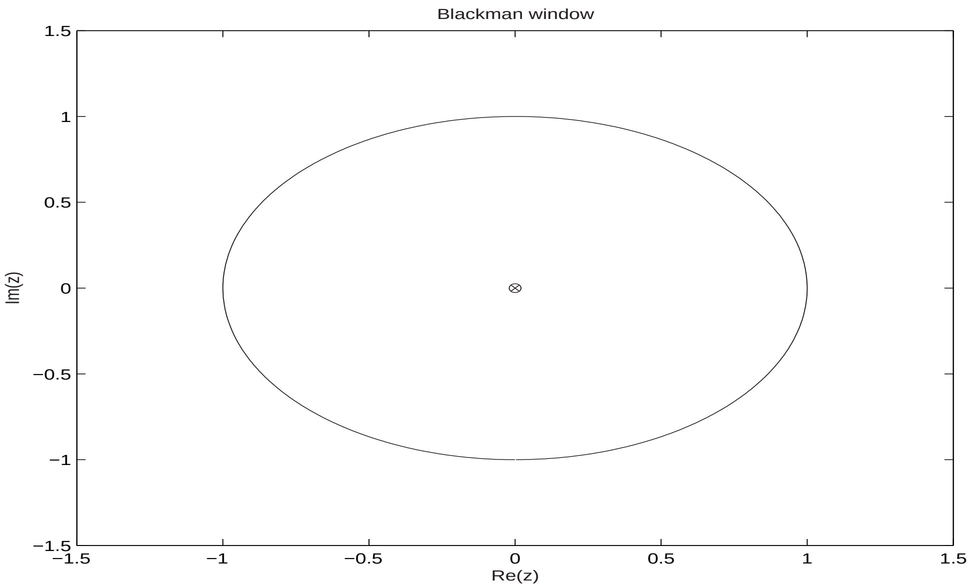

Figure 32: Blackman window, pole zero diagram

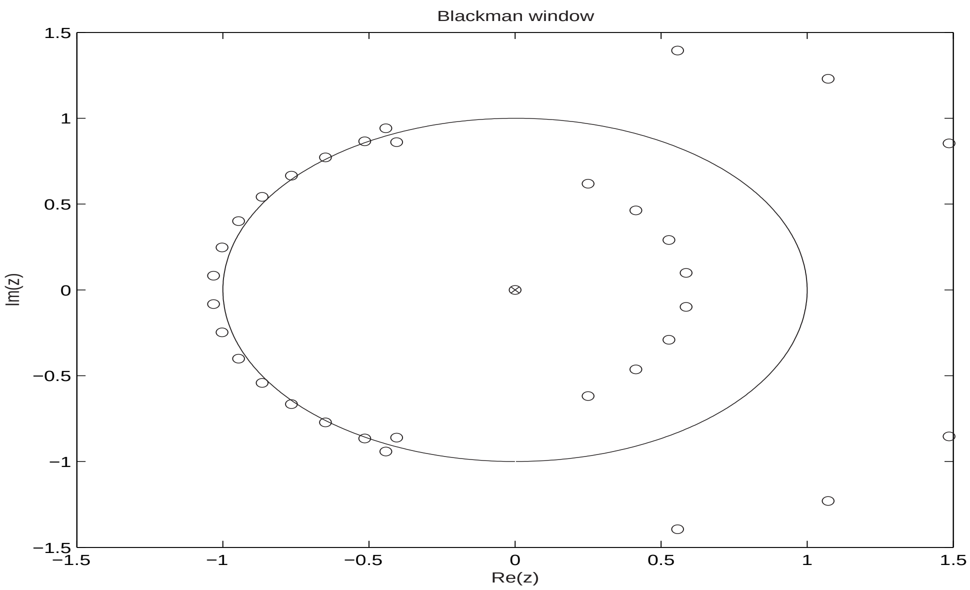

Figure 33: Blackman window, pole zero diagram ($f_c = 1995$)

Question 19

I used Matlab to calculate the frequency response of the three fir digital filters, which simplified matters until I tried to calculate the phase of the filters. This returned a sharply discontinuous phase response graph, with Matlab automatically cycling values within a range of $[-\pi \ldots \pi]$. The unwrap function, which was previously used to successfully maintain phase progression information under the iir filters, could not cope with the steep phase shift inherent to the filter. I had to write my own very rudimentary unwrap script (donunroll3), which was limited (very) to use with linearly varying phases. (Which the initial plots of the discontinuous phase revealed it to be.)

The gain and phase are plotted around the unit circle in the s plane. This unit circle in the s plane is related to the frequency plane by :

$$\begin{aligned} \omega &= \frac{\Omega}{T_{sample}} \\ 2\pi f &= \Omega f_{sample} \\ f &= \frac{\Omega f_{sample}}{2\pi} \\ \text{Where } \Omega &= [-\pi \ldots \pi] \\ \therefore f &= [-4000 \ldots 4000] \end{aligned}$$

All the FIR filters were discovered to have linear phase response. Gibbs phenomenon is normally associated with sudden cutoffs in the frequency domain resulting in a ripple in the time domain. The sudden cutoffs applied by our different windowing functions, in sampling the impulse response, induce similar rippling in the frequency domain. This effect is incredibly pronounced in the rectangular window filter, and results in a strong ripple at the edge of the passband. It results in a barely perceivable waver in the passband when using the Hamming window and in absent in the passband when using the Blackman window.

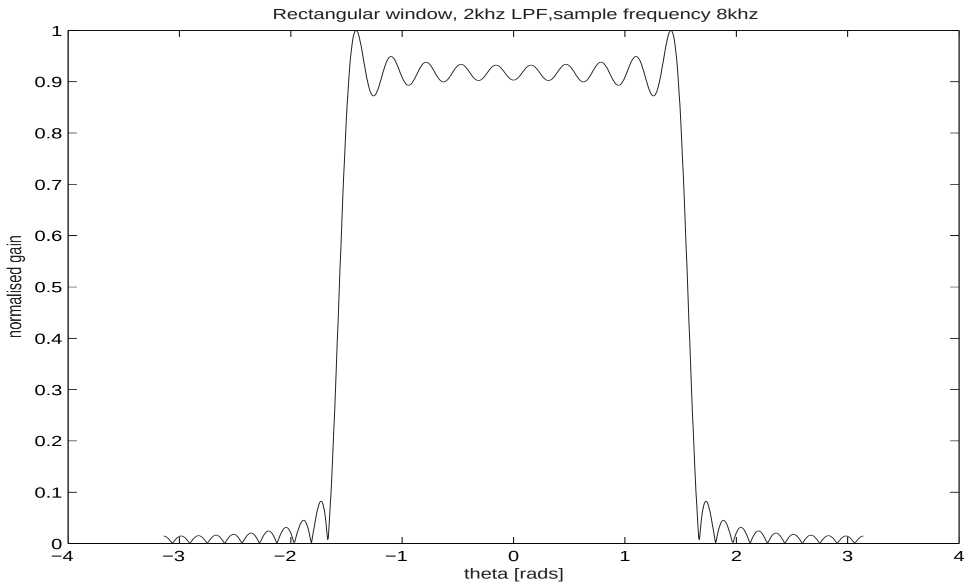

Figure 34: Rectangular window, digital filter normalised gain

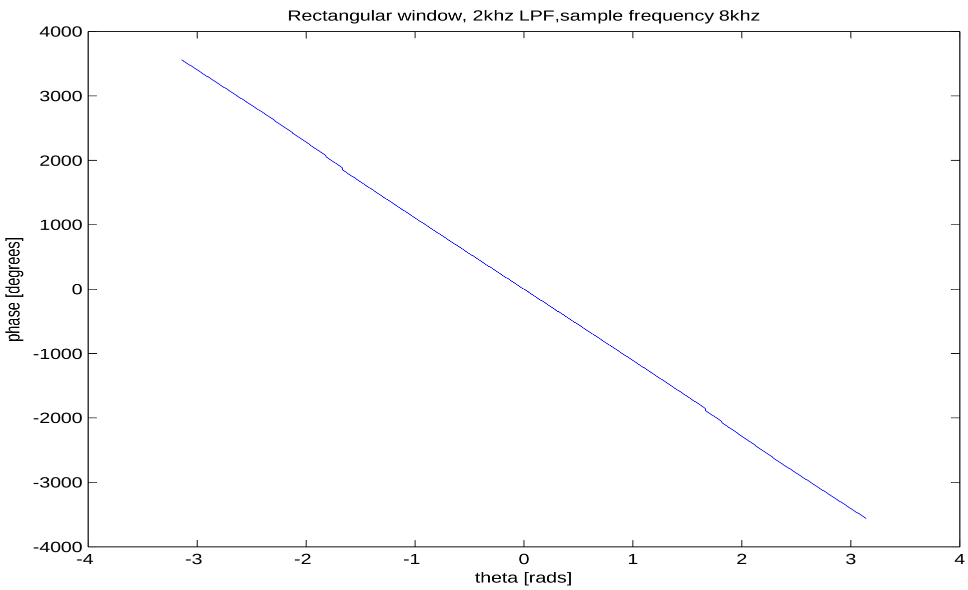

Figure 35: Rectangular window, digital filter phase response

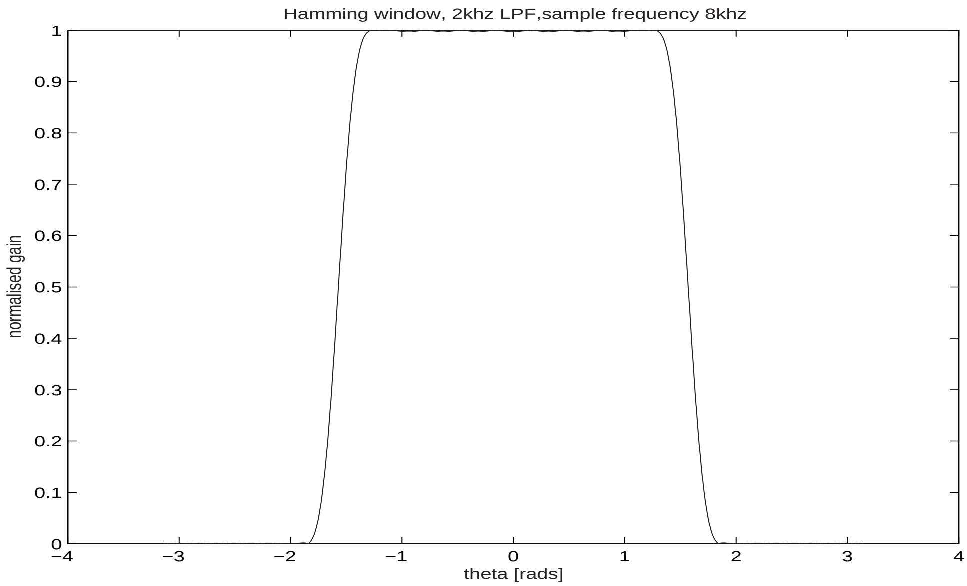

Figure 36: Hamming window, digital filter normalised gain

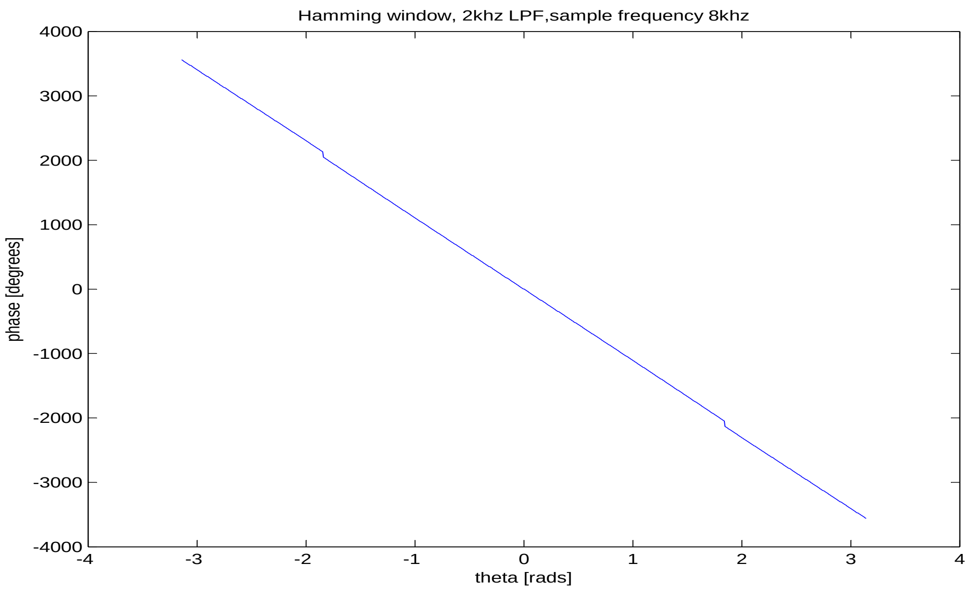

Figure 37: Hamming window, digital filter phase response

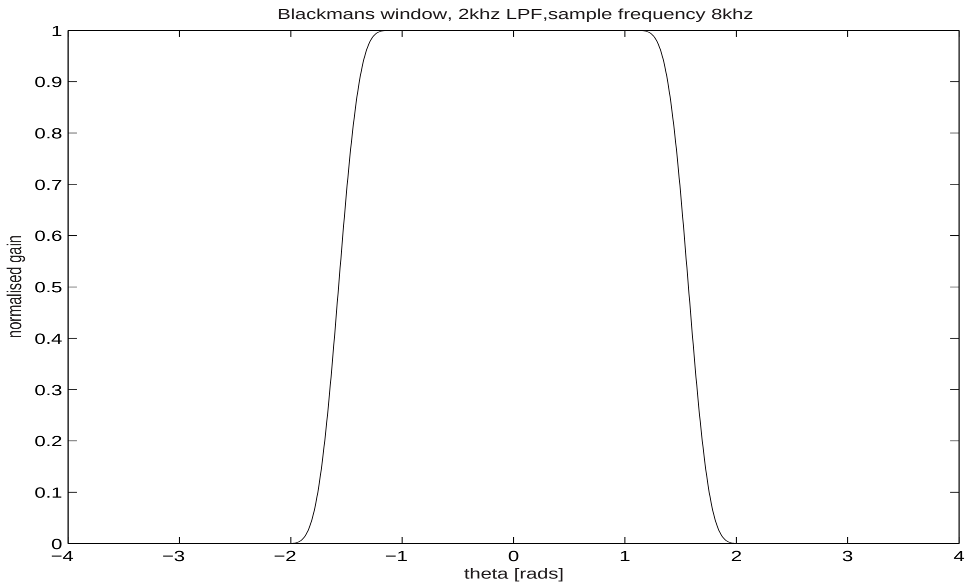

Figure 38: Blackman window, digital filter normalised gain

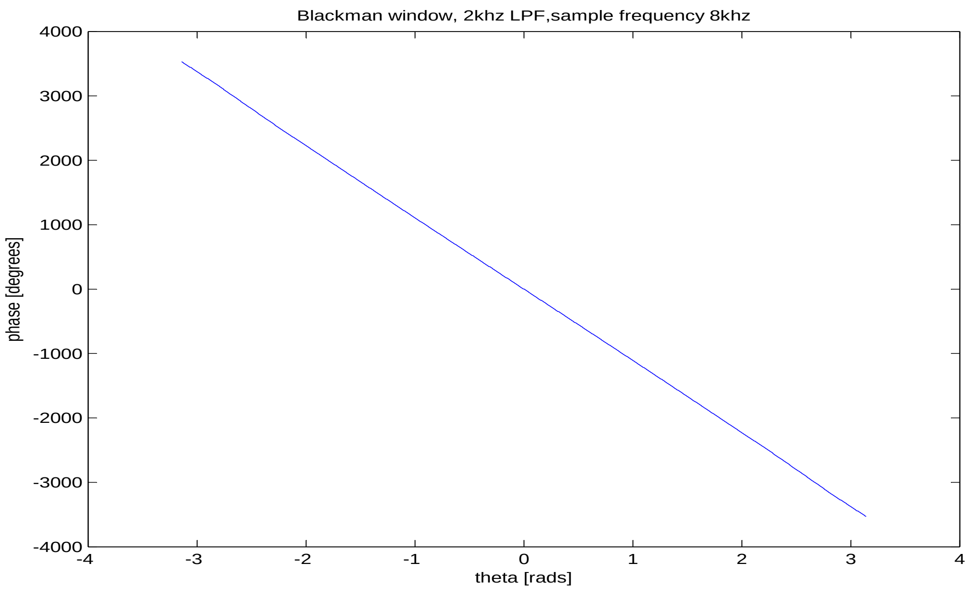

Figure 39: Blackman window, digital filter phase response

It became apparent in the later comparison of implementation vs theory, that the graphs offer far more information when the gain was displayed in decibels. The graphs below clearly show the ripple at the edge of the passband, moving away from the passband as we progress from the rectangular window to the Blackman window. Gibbs phenomena can not avoided, but the more advanced windowing methods shift the oscillation away from the passband, where they have a greatly diminished effect on the filtering process.

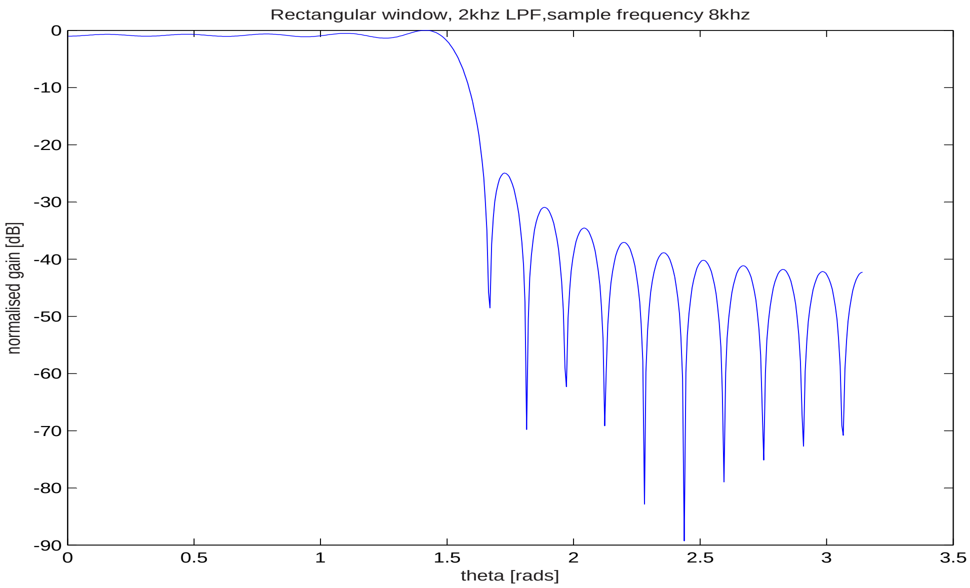

Figure 40: Rectangular window, digital filter normalised gain in dB

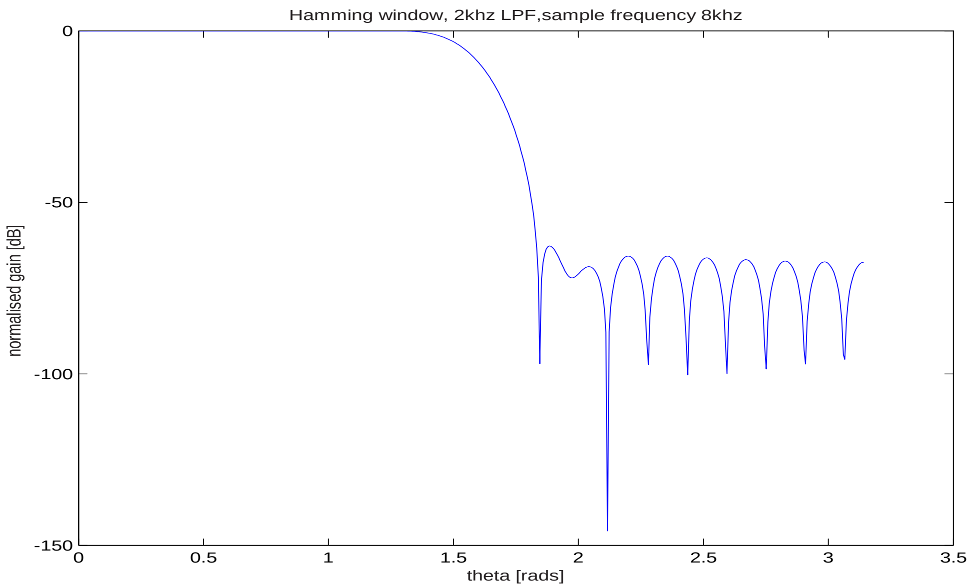

Figure 41: Hamming window, digital filter normalised gain in dB

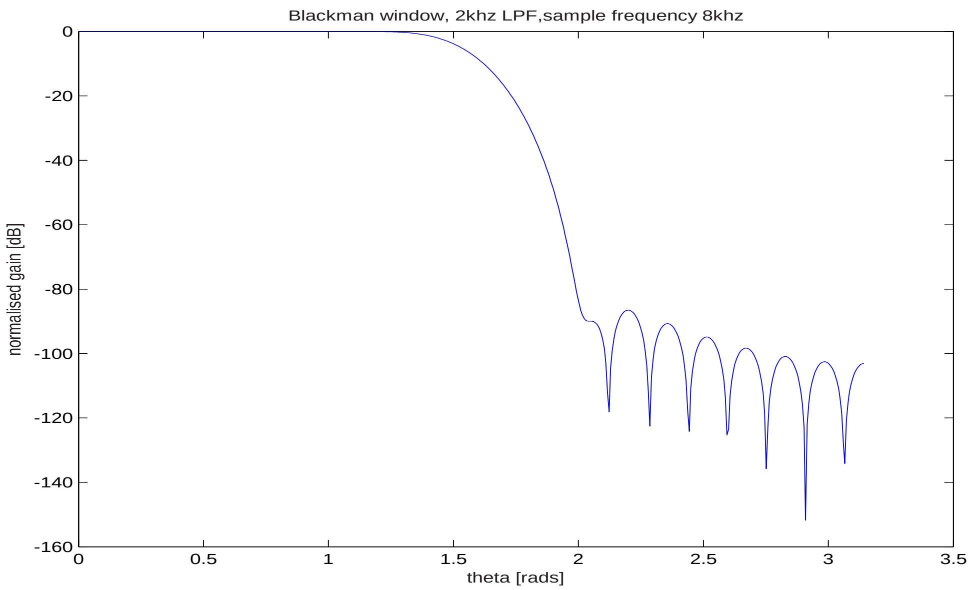

Figure 42: Blackman window, digital filter normalised gain in dB